

Global MHD Simulations: Nuts and Bolts

Joachim Raeder

*Institute of Geophysics and Planetary Physics
University of California, Los Angeles*

Outline

- Some history of global modeling
- Geometry and grids
- Equations
- Initial and boundary conditions
- Ionosphere model
- MHD solver – algorithms
- Validation
- Computing issues
- To do list

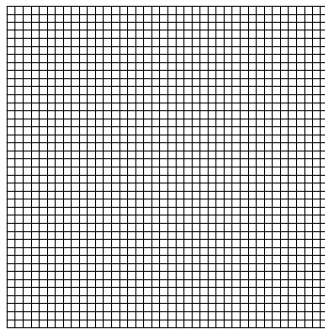
A Brief History of Global MHD Simulations

- 1978: First 2d simulations by Leboeuf et al. (so we are close to the 20th anniversary).
- Early 80's: First 3d simulations (Brecht, Lyon, Wu, Ogino).
- Late 80's: Model refinements (FACs, ionosphere, higher resolution, fewer symmetries).
- Early 90's: Long geomagnetic tails, refined ionosphere models.
- Mid 90's: ISTP is well underway, modeling has become part of the missions, first comparisons with *in situ* space observations and ground based observations. Beginning of *quantitative* modeling.
- Late 90's: Global modeling has become an integrated part of many experimental studies. Models provide an extension to spatially limited observations and help us to understand the physics.

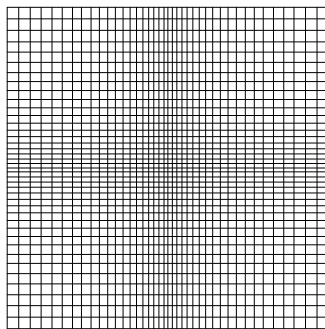
Simulation geometry and grid

- Simulation boundaries should be in supermagnetosonic flows, i.e., $\geq 18 R_E$ from Earth on the sunward side, $\geq 200 R_E$ in the tailward direction, and $\geq 50 R_E$ in the transverse directions.
- Numerical grids:

⇒ uniform cartesian: lowest programming overhead, lowest computing overhead, no memory overhead, easiest parallelization, near perfect load balancing, not adaptable

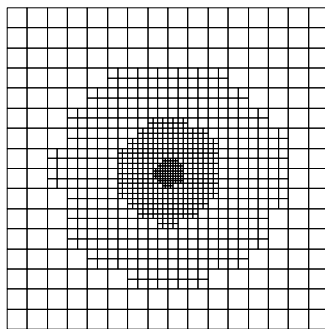


⇒ stretched cartesian: low programming overhead, low computing overhead, no memory overhead, easiest parallelization, near perfect load balancing, somewhat adaptable

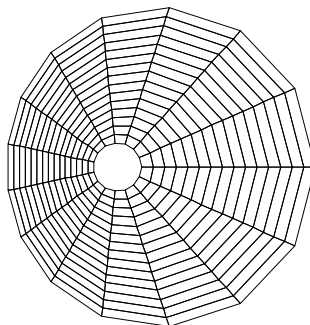


grids (continued)

⇒ nested cartesian (can be self-adapting): medium to high programming overhead, small computing overhead, medium memory overhead, difficult to parallelize and load balance, internal discontinuities, very adaptable

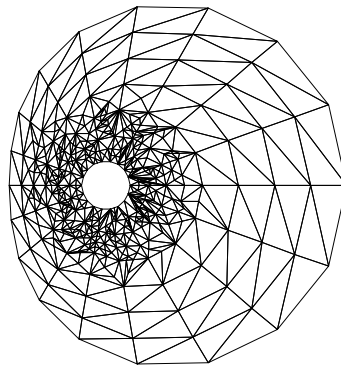


⇒ non-cartesian with regular topology: medium programming overhead, small computing overhead, low memory overhead, parallelizes and load balances like regular cartesian grid, somewhat adaptable

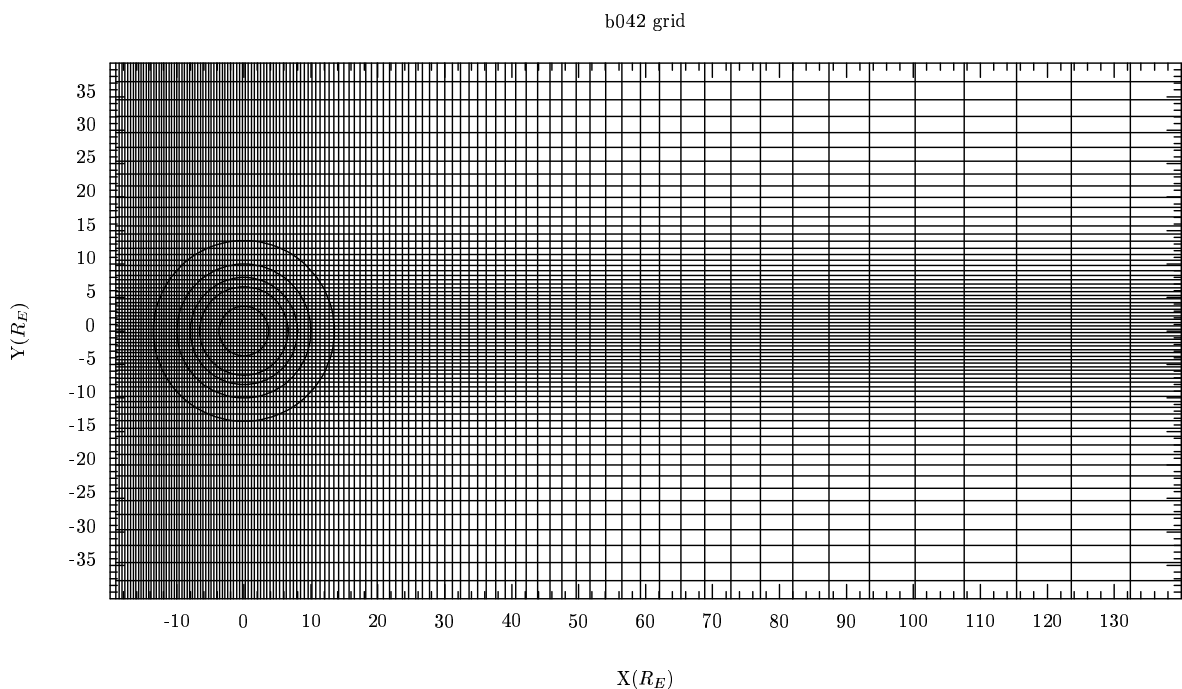


grids (continued)

⇒ non-cartesian with irregular topology (can be self-adapting):
high programming overhead, high computing overhead, high
memory overhead, difficult to parallelize and load balance,
smooth internal transitions, very adaptable, can use FEM
technology



⇒ UCLA-GGCM grid:



Equations

- non-conservative (primitive variables)

$$\begin{aligned}\frac{\partial \rho}{\partial t} &= -\nabla \cdot (\rho \mathbf{v}) \\ \frac{\partial \mathbf{v}}{\partial t} &= -(\mathbf{v} \cdot \nabla) \mathbf{v} - \left(\frac{1}{\rho}\right) \nabla p + \left(\frac{1}{\rho}\right) \mathbf{j} \times \mathbf{B} \\ \frac{\partial p}{\partial t} &= -(\mathbf{v} \cdot \nabla) p - \gamma p \nabla \cdot \mathbf{v} \\ \frac{\partial \mathbf{B}}{\partial t} &= -\nabla \times \mathbf{E} \\ \nabla \cdot \mathbf{B} &= 0 \\ \mathbf{E} &= -\mathbf{v} \times \mathbf{B} + \eta \mathbf{j} \\ \mathbf{j} &= \nabla \times \mathbf{B}\end{aligned}$$

⇒ no strict numerical conservation of momentum and energy possible

⇒ numerical difficulties with convective derivatives

⇒ leads to numerical difficulties with strong shocks, errors in RH conditions and shock speed

Equations (continued)

- full conservative

$$\begin{aligned}
 \frac{\partial \rho}{\partial t} &= -\nabla \cdot (\rho \mathbf{v}) \\
 \frac{\partial \rho \mathbf{v}}{\partial t} &= -\nabla \cdot \left\{ \rho \mathbf{v} \mathbf{v} + p \underline{\underline{\mathbf{I}}} - \left(\mathbf{B} \mathbf{B} - \frac{1}{2} B^2 \underline{\underline{\mathbf{I}}} \right) \right\} \\
 \frac{\partial U}{\partial t} &= -\nabla \cdot \left\{ (U + p) \mathbf{v} + \mathbf{E} \times \mathbf{B} \right\} \\
 \frac{\partial \mathbf{B}}{\partial t} &= -\nabla \times \mathbf{E} \\
 \nabla \cdot \mathbf{B} &= 0 \\
 \mathbf{E} &= -\mathbf{v} \times \mathbf{B} + \eta \mathbf{j} \\
 \mathbf{j} &= \nabla \times \mathbf{B} \\
 p &= (\gamma - 1) \left\{ U - \frac{1}{2} \rho v^2 - \frac{1}{2} B^2 \right\}
 \end{aligned}$$

⇒ allows strict numerical conservation of mass, momentum and energy

⇒ numerical difficulties in low β regions (negative pressure possible because p becomes difference of large numbers)

Equations (continued)

- Gas dynamic conservative

$$\begin{aligned}\frac{\partial \rho}{\partial t} &= -\nabla \cdot (\rho \mathbf{v}) \\ \frac{\partial \rho \mathbf{v}}{\partial t} &= -\nabla \cdot (\rho \mathbf{v} \mathbf{v} + p \underline{\underline{\mathbf{I}}}) + \mathbf{j} \times \mathbf{B} \\ \frac{\partial e}{\partial t} &= -\nabla \cdot (\{e + p\} \mathbf{v}) + \mathbf{j} \cdot \mathbf{E} \\ \frac{\partial \mathbf{B}}{\partial t} &= -\nabla \times \mathbf{E} \\ \nabla \cdot \mathbf{B} &= 0 \\ \mathbf{E} &= -\mathbf{v} \times \mathbf{B} + \eta \mathbf{j} \\ \mathbf{j} &= \nabla \times \mathbf{B} \\ p &= (\gamma - 1) \left\{ e - \frac{1}{2} \rho v^2 \right\}\end{aligned}$$

⇒ compromise

⇒ allows strict numerical conservation of mass, momentum and plasma energy, but no strict conservation of total energy

⇒ low β regions pose no difficulty

⇒ could be combined with full conservative scheme by integrating both energy equations and using a ' β switch'

Anomalous resistivity

- Current driven instabilities:

⇒ ion sound instability:

$$\eta \sim (c/\omega_e)^2 \omega_i (v_D/c_s) (T_e/T_i)$$

⇒ electron–cyclotron drift instability:

$$\eta \sim r_e^2 \Omega_e (v_D/v_e)^3$$

⇒ lower hybrid drift instability:

$$\eta \sim r_e^2 (m_i/m_e) (v_D/v_e)^2 \omega_{lh}$$

⇒ MTSI/KCSI/IWI:

$$\nu_c/\Omega_i \approx 0.005 - 0.08 \quad \eta \approx 10^{-7} \text{ to } 2 \times 10^{-5} \text{ s}$$

⇒ simulation studies [Tanaka, Brackbill]: $\eta \sim v_D^2$

⇒ observations [Cattell et al.]: $R_m \approx 0.1 \dots 10$

⇒ most known anomalous resistivity models predict $\eta \sim j^p$
with $p = 2$ the most likely value

- Parameterization:

$$\eta = \alpha j'^2 \quad \text{if } j' \geq \delta, \quad 0 \text{ otherwise} \quad (1)$$

$$j' = \frac{|j|\Delta}{|B| + \epsilon} \quad (2)$$

Boundary conditions

- Sunward side:

⇒ Arbitrary fixed or time dependent

⇒ Measured solar wind data

⇒ Problem with B_x : Three dimensional structure of the solar wind needs to be known because

$$\nabla \cdot \mathbf{B} = 0 \iff \mathbf{n} \cdot (B_{upstream} - B_{downstream}) = 0$$

⇒ implies that $B_x = B_n$ cannot change if solar wind parameters are independent of Y and Z.

⇒ solution: find \mathbf{n} , difficult with single solar wind monitor, boundary normal methods (minimum variance, ...) can be applied

- All other sides:

⇒ free flow conditions for plasma and transverse B components:

$$\frac{\partial \Psi}{\partial \mathbf{n}} = 0$$

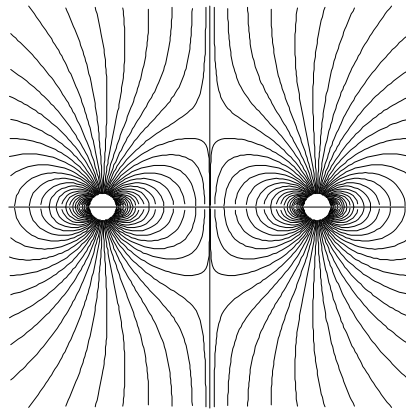
⇒ normal component of B: follows from $\nabla \cdot \mathbf{B} = 0$

- Inner boundary (ionosphere): later

Initial conditions

- Magnetic field:

Superposition of dipole with mirror dipole to create $B_x = 0$ surface sunward of Earth, then replace field on sunward side with initial solar wind field.

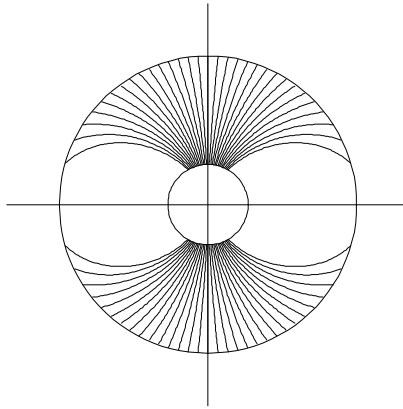


- plasma:

cold ($5000 \text{ } ^\circ\text{K}$), tenuous (0.1cm^{-3}), uniform

Ionosphere model

- Geometry and mapping:
pick field aligned currents (j_{\parallel}), at the inner boundary ($2 - 4 R_E$) from the MHD grid and map along dipole field lines onto the ionosphere:



- covers latitudes from 58° to 90° .
- very high v_A inside inner boundary, solving the MHD equations is not necessary.
- Use mapped FAC, precipitation parameters to solve for the ionospheric potential Φ .
- Map potential back to inner boundary and use as boundary condition for flow:

$$\mathbf{v} = \frac{(-\nabla\Phi) \times \mathbf{B}}{|\mathbf{B}|^2}$$

Ionosphere model (continued)

- Limiting cases:

$\Rightarrow \Phi = 0 \implies \mathbf{E} = 0 \implies \mathbf{v} = 0$ (equivalent to infinite ionospheric conductance): field lines are tied in the ionosphere, no convection in the ionosphere, and convection in the magnetosphere inhibited.

$\Rightarrow j_{\parallel} \rightarrow 0$ (zero conductance): Field lines slip free through the ionosphere and Earth.

\Rightarrow in reality the ionosphere has a finite conductance and field lines are dragged through the ionospheric plasma, dissipating energy.

- Potential equation, solved on each hemisphere separately:

$$\nabla \cdot \underline{\underline{\Sigma}} \cdot \nabla \Phi = -j_{\parallel} \sin I$$

- Boundary condition: $\Phi(\text{equator})=0$.

- Conductance tensor:

$$\underline{\underline{\Sigma}} = \begin{pmatrix} \Sigma_{\theta\theta} & \Sigma_{\theta\lambda} \\ -\Sigma_{\theta\lambda} & \Sigma_{\lambda\lambda} \end{pmatrix}$$

$$\Sigma_{\theta\theta} = \frac{\Sigma_P}{\sin^2 I} \quad , \quad \Sigma_{\theta\lambda} = \frac{\Sigma_H}{\sin I} \quad , \quad \Sigma_{\lambda\lambda} = \Sigma_P$$

Ionosphere model (continued)

- Ionospheric conductances, 3 primary sources:

⇒ Solar EUV [*Moen and Brekke, 1993*]:

$$\begin{aligned}\Sigma_H &= F_{10.7}^{0.53} (0.81 \cos \chi + 0.54 \cos^{1/2} \chi) \\ \Sigma_P &= F_{10.7}^{0.49} (0.34 \cos \chi + 0.93 \cos^{1/2} \chi)\end{aligned}$$

⇒ Parallel potential drops [*Knight, 1973; Lyons et al., 1979*]:

$$\Delta\Phi = K \max(0, -j_{\parallel})$$

$$K = \frac{e^2 n_e}{\sqrt{2\pi m_e k T_e}}$$

⇒ Electron acceleration:

$$F_E = \Delta\Phi_{\parallel} j_{\parallel} \quad , \quad E_0 = e\Delta\Phi_{\parallel}$$

⇒ Pitch angle scattering:

$$F_E = n_e (kT_e / 2\pi m_e)^{\frac{1}{2}} \quad , \quad E_0 = kT_e$$

⇒ Hall, Pedersen conductance from e - precipitation: [*Hardy et al., 1987*]:

$$\begin{aligned}\Sigma_P &= [40E_0 / (16 + E_0^2)] F_E^{1/2} \\ \Sigma_H &= 0.45 E_0^{5/8} \Sigma_P\end{aligned}$$

MHD numerics

- Time differencing

⇒ Model equation:

$$\frac{\partial U}{\partial t} = -\nabla \cdot \mathbf{F}(U)$$

⇒ Explicit time differences, predictor - corrector scheme (second order accurate):

$$U^{n+\frac{1}{2}} = U^n - \frac{1}{2}\Delta t \nabla \cdot \mathbf{F}(U^n)$$

$$U^{n+1} = U^n - \Delta t \nabla \cdot \mathbf{F}(U^{n+\frac{1}{2}})$$

⇒ Explicit time differences, leap - frog scheme (second order accurate):

$$U^{n+1} = U^{n-1} - 2\Delta t \nabla \cdot \mathbf{F}(U^n, U^{n-1})$$

⇒ Stability criterion (Courant-Fridrichs-Levy, CFL):

$$\Delta t_{max} \leq \delta \frac{\min(\Delta x, \Delta y, \Delta z)}{|\mathbf{v}| + v_{MS}}$$

⇒ CFL criterion can be very restrictive, Δt_{max} must be satisfied everywhere in the simulation domain

⇒ Implicit time differencing schemes:

$$U^{n+1} = U^{n-1} - \Delta t \nabla \cdot \mathbf{F}(U^{n+1}, U^n, U^{n-1}, \dots)$$

⇒ Implicit time differencing can be unconditionally stable, but generally requires the solution of large linear systems, too expensive and impracticable

MHD numerics (continued)

- Spatial discretization:

⇒ Finite differences (FD).

⇒ Finite volume (FD), reduces to FD on cartesian grids.

⇒ Finite element (FEM), mostly used for non - cartesian irregular grids.

- Conservative FD:

⇒ Model equation:

$$\frac{\partial U}{\partial t} = -\nabla \cdot \mathbf{F}(U)$$

⇒ discretize as:

$$\begin{aligned} \frac{\partial U}{\partial t} = & - (f_{i+\frac{1}{2},j}(U) - f_{i-\frac{1}{2},j}(U)) / \Delta x \\ & - (f_{i,j+\frac{1}{2}}(U) - f_{i,j-\frac{1}{2}}(U)) \Delta y \end{aligned}$$

⇒ numerical fluxes:

$$f_{i+\frac{1}{2},j} = G(\dots, U_{i-1,j}, U_{i,j}, U_{i+1,j}, \dots)$$

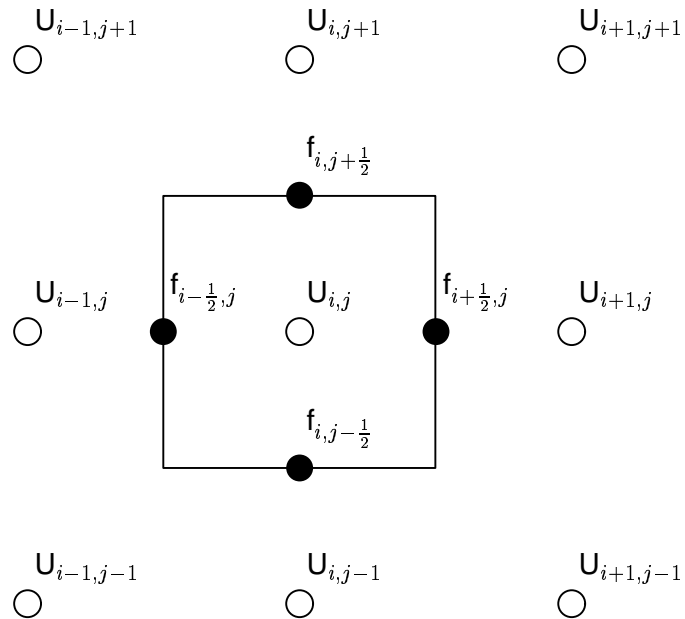
$$f_{i,j+\frac{1}{2}} = G(\dots, U_{i,j-1}, U_{i,j}, U_{i,j+1}, \dots)$$

⇒ numerical fluxes must be consistent with the physical flux $F(U)$:

$$G(U, \dots, U, U, \dots, U) = F(U)$$

MHD numerics (continued)

- Schematic of conservative FD:



- This differencing is equivalent to (and therefore conservative):

$$\frac{\partial}{\partial t} \iiint_V U dV = \iint_S \mathbf{F} ds$$

MHD numerics (continued)

- Examples of numerical fluxes:

⇒ second order central:

$$f_{i+\frac{1}{2}} = \frac{1}{2}(F(U_i) + F(U_{i+1}))$$

⇒ fourth order central:

$$f_{i+\frac{1}{2}} = \frac{7}{12}(F(U_i) + F(U_{i+1})) - \frac{1}{12}(F(U_{i-1}) + F(U_{i+2}))$$

⇒ Lax scheme:

$$f_{i+\frac{1}{2}} = \frac{1}{2}(F(U_i) + F(U_{i+1})) - \frac{1}{2}(U_{i+1} - U_i)$$

⇒ Two step Lax Wendroff scheme: Use Lax scheme for predictor, and second order central for corrector.

⇒ Rusanov scheme:

$$f_{i+\frac{1}{2}} = \frac{1}{2}(F(U_i) + F(U_{i+1})) - \frac{1}{4}(|v_i| + |v_{i+1}| + c_i + c_{i+1})(U_{i+1} - U_i)$$

⇒ Godunov schemes: solve a Riemann problem (i.e. the decay of a step function into waves) at the cell interface and compute the fluxes directly from the wave propagation. Accurate for gas-dynamics, but difficulties in MHD: degenerate eigenvector because of $\nabla \cdot \mathbf{B} = 0$.

MHD numerics (continued)

- Error terms:

$$\begin{aligned}\Delta x \frac{\partial U}{\partial t} &= -(f_{i+\frac{1}{2}} - f_{i-\frac{1}{2}}) \\ &+ a_1(\Delta x)^2 \frac{\partial^2}{\partial x^2} F(U) + b_1(\Delta x)^3 \frac{\partial^3}{\partial x^3} F(U) \\ &+ a_2(\Delta x)^4 \frac{\partial^4}{\partial x^4} F(U) + b_2(\Delta x)^5 \frac{\partial^5}{\partial x^5} F(U) \\ &+ \dots\end{aligned}$$

⇒ error terms with even derivatives cause diffusion

⇒ error terms with odd derivatives cause dispersion

⇒ central difference schemes have no diffusion, but dispersion, big problem at shocks and discontinuities

⇒ first order schemes are less dispersive, but very diffusive

⇒ see examples: wiggles at discontinuities

- Monotonicity: A scheme is called monotone if it lets no new extrema develop in the solution (that is exactly what we want).

MHD numerics (continued)

- Harten's (Di)Lemma:

A monotone scheme is at most first order accurate!

Thus, a globally monotone scheme will always be very diffusive.

- Solution to Harten's (Di)Lemma:

Hybridize the numerical fluxes: Use first order numerical flux (f^l) where a new extremum might develop (like at a shock), and use high order fluxes (f^h) where the solution is smooth.

$$f_{i+\frac{1}{2}} = \theta_{i+\frac{1}{2}} f_{i+\frac{1}{2}}^h + (1 - \theta_{i+\frac{1}{2}}) f_{i+\frac{1}{2}}^l$$

⇒ Obviously, $0 \leq \theta \leq 1$. θ can be a function of anything, but generally depends on gradients of the solution.

- The switch function θ is called *Flux Limiter*. There is no optimal flux limiter. A few choices:

⇒ Hartens “edge condition” flux limiter

⇒ vanLeer's flux limiter

⇒ Flux Corrected Transport (FCT)

⇒ Total Variance Diminishing (TVD) schemes (the monotonicity constraint is somewhat relaxed)

⇒ ...

MHD numerics (continued)

- Keeping divergence of \mathbf{B} zero

$\Rightarrow \nabla \cdot \mathbf{B} = 0$ is an initial condition, $\nabla \cdot \mathbf{B}$ is conserved by Faraday's law:

$$\nabla \cdot \frac{\partial \mathbf{B}}{\partial t} = \frac{\partial(\nabla \cdot \mathbf{B})}{\partial t} = -\nabla \cdot \nabla \times \mathbf{E} = 0$$

$\Rightarrow \nabla \cdot \mathbf{B}$ cleaning, projection method: solve

$$\nabla^2 \Psi = -(\nabla \cdot \mathbf{B})$$

and correct the field:

$$\mathbf{B}' = \mathbf{B} + \nabla \Psi$$

requires the numerical solution of a Poisson equation (expensive). Can only be as good as the solution of Ψ .

$\Rightarrow \nabla \cdot \mathbf{B}$ convection: Effectively modify equations so that $\nabla \cdot \mathbf{B}$ convects through the system (Gombosi):

$$\frac{d(\nabla \cdot \mathbf{B})}{dt} = 0$$

$\nabla \cdot \mathbf{B}$ must convect out of the system (inner magnetosphere?).

\Rightarrow Use numerical $\nabla \cdot$ and $\nabla \times$ operators with $\nabla \cdot \nabla \times \Psi = 0$

\Rightarrow Use a magnetic flux conservative scheme that keeps $\nabla \cdot \mathbf{B} = 0$ to roundoff error.

MHD numerics (continued)

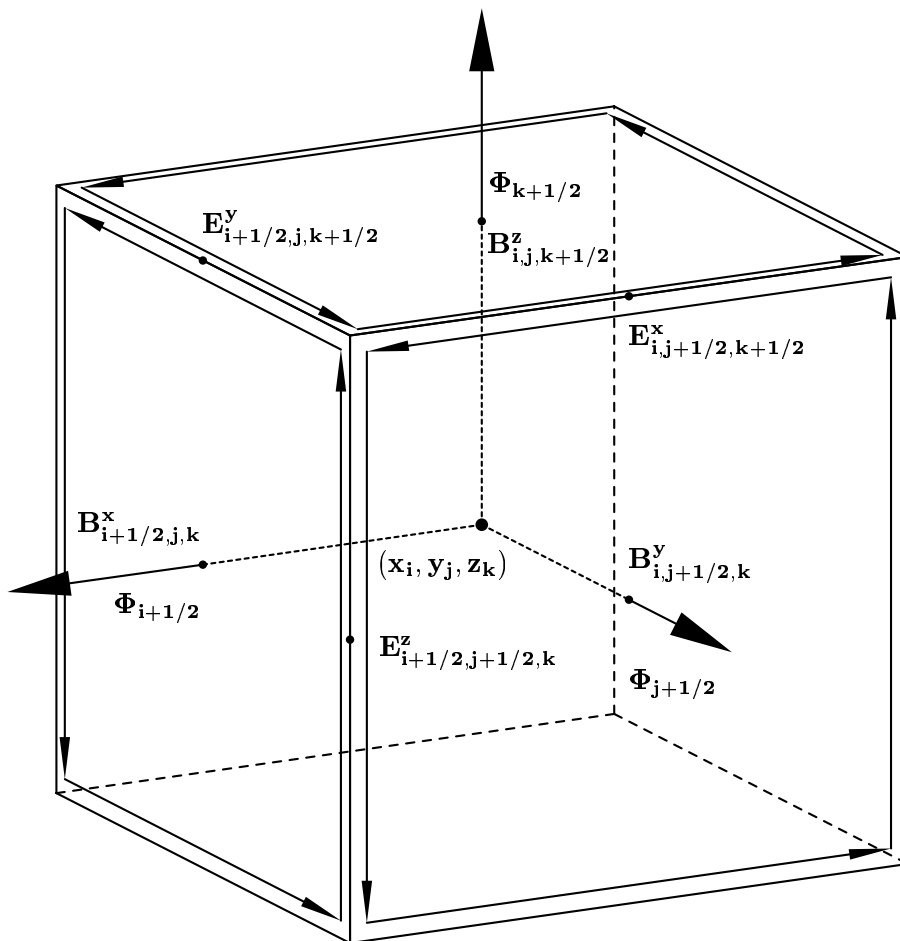
⇒ magnetic flux conservative scheme (continued)
 place the magnetic field components on the center of cell faces:

$$(B_x)_{i+\frac{1}{2},j,k}, (B_y)_{i,j+\frac{1}{2},k}, (B_z)_{i,j,k+\frac{1}{2}}$$

⇒ and the electric field (a numerical flux) on the centers of the cell edges:

$$(E_x)_{i,j+\frac{1}{2},k+\frac{1}{2}}, (E_y)_{i+\frac{1}{2},j,k+\frac{1}{2}}, (E_z)_{i+\frac{1}{2},j+\frac{1}{2},k}$$

[Evans and Hawley, 1987].



MHD numerics (continued)

⇒ magnetic flux conservative scheme (continued)
then:

$$\begin{aligned} \frac{\partial}{\partial t}(B_x)_{i+\frac{1}{2},j,k} = & \\ & \{(E_y)_{i+\frac{1}{2},j,k+\frac{1}{2}} - (E_y)_{i+\frac{1}{2},j,k-\frac{1}{2}}\}/\Delta z \\ & - \{(E_z)_{i+\frac{1}{2},j+\frac{1}{2},k} - (E_z)_{i-\frac{1}{2},j+\frac{1}{2},k}\}/\Delta y \end{aligned}$$

⇒ analogous for B_y and B_z

⇒ By advancing the field components in this way on all 6 cell faces and summing up it follows:

$$\begin{aligned} \frac{\partial}{\partial t} \int \int_{cell} \Phi df = & \\ = \Delta y \Delta z \left(\frac{\partial B_x}{\partial t} \right)_{i-\frac{1}{2}} + \Delta y \Delta z \left(\frac{\partial B_x}{\partial t} \right)_{i+\frac{1}{2}} + \Delta x \Delta z \left(\frac{\partial B_y}{\partial t} \right)_{j+\frac{1}{2}} + \dots & \\ = \{((E_y)_{i+\frac{1}{2},j,k+\frac{1}{2}} - (E_y)_{i+\frac{1}{2},j,k-\frac{1}{2}}) + & \\ ((E_y)_{i+\frac{1}{2},j,k-\frac{1}{2}} - (E_y)_{i+\frac{1}{2},j,k-\frac{1}{2}}) + \dots\} \Delta x \Delta y \Delta z & \\ = 0 & \end{aligned}$$

thus $\Phi = \text{const.}$

⇒ The field can be initialized divergence free by using a vector potential \mathbf{A} in place of \mathbf{E} .

MHD numerics (continued)

- How to handle stretched grids:

⇒ grid coordinates given by analytic function:

$x(i, j, k)$, $y(i, j, k)$, $z(i, j, k)$, then:

$$\begin{aligned}\frac{\partial}{\partial x} F(x, y, z) &= \\ &= \frac{\partial F}{\partial i} \frac{\partial i}{\partial x} + \frac{\partial F}{\partial j} \frac{\partial j}{\partial x} + \frac{\partial F}{\partial k} \frac{\partial k}{\partial x} \\ &= \frac{\partial F}{\partial i} \left(\frac{\partial i}{\partial x} \right)^{-1} + \frac{\partial F}{\partial j} \left(\frac{\partial j}{\partial x} \right)^{-1} + \frac{\partial F}{\partial k} \left(\frac{\partial k}{\partial x} \right)^{-1}\end{aligned}$$

⇒ analogous for y and z derivative.

⇒ particularly simple for stretched grid:

$$\frac{\partial}{\partial x} F(x, y, z) = \frac{\partial F}{\partial i} \left(\frac{\partial i}{\partial x} \right)^{-1}$$

$$\frac{\partial}{\partial y} F(x, y, z) = \frac{\partial F}{\partial j} \left(\frac{\partial j}{\partial y} \right)^{-1}$$

$$\frac{\partial}{\partial z} F(x, y, z) = \frac{\partial F}{\partial k} \left(\frac{\partial k}{\partial z} \right)^{-1}$$

Validation

- Compare with non-trivial solutions of the MHD equations (few available):

⇒ shock tube problems (check for RH conditions, expansion shocks, flux limiters). Table of shock tube parameters used by ISTP:

ρ_1	ρ_2	p_1	p_2	v_{x1}	v_{x2}	v_{y1}	v_{y2}	v_{z1}	v_{z2}	B_{x1}	B_{x2}	B_{y1}	B_{y2}	B_{z1}	B_{z2}	γ
1	0.125	1	0.1	0	0	0	0	0	0	0	0	0	0	0	0	1.4
1	0.125	100	0.1	0	0	0	0	0	0	0	0	0	0	0	0	1.4
1	0.125	1	0.1	0	0	0	0	0	0	0.75	0.75	0	0	1	-1	2
1	0.125	1	0.1	0	0	0	0	0	0	0	0	10	0.5	10	0.5	2
1	0.125	100	0.1	0	0	0	0	0	0	0.75	0.75	0	0	1	-1	2
1	0.125	100	0.1	0	0	0	0	0	0	0	0	10	0.5	10	0.5	2
1	0.125	1	0.1	0	0	0	0	0	0	0	0	0	0	0.1	0.1	2

⇒ 2D/3D self-similar solutions by Low [1982, Ap. J].

- **B** convection test to evaluate $\nabla \cdot \mathbf{B} = 0$: initialize a non-trivial **B** field from $\nabla \times \mathbf{A}$ such that $\mathbf{B} = 0$ in most of the domain (magnetic bubble) and convect with $\mathbf{V} = (V_x, 0, 0)$. $\nabla \cdot \mathbf{B} = 0$ violation will become evident by B_x sticking to the grid:

$$\frac{\partial \mathbf{B}}{\partial t} = -\nabla \times \mathbf{E}$$

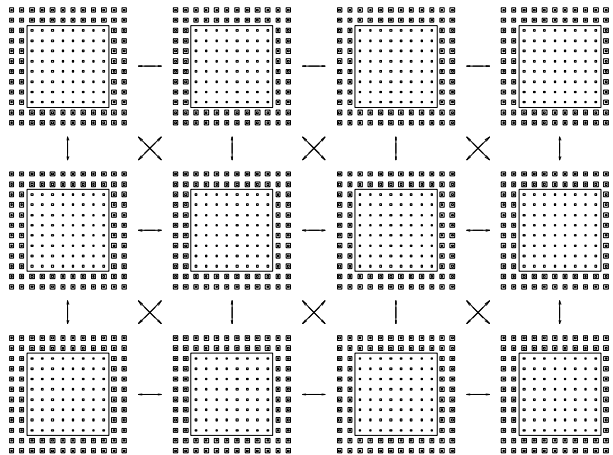
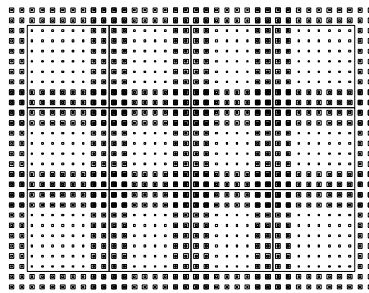
$$\Rightarrow \frac{d\mathbf{B}}{dt} = \mathbf{V}(\nabla \cdot \mathbf{B})$$

- Convergence test: run same problem twice: with highest resolution possible and with factor two lower resolution. The results should be qualitatively the same and quantitatively similar.
- Reality test: drive model with observed solar wind and IMF and compare results with *in situ* observations.

Computer issues

- Parallel implementation on MIMD (Multiple Instruction - Multiple Data) computers:

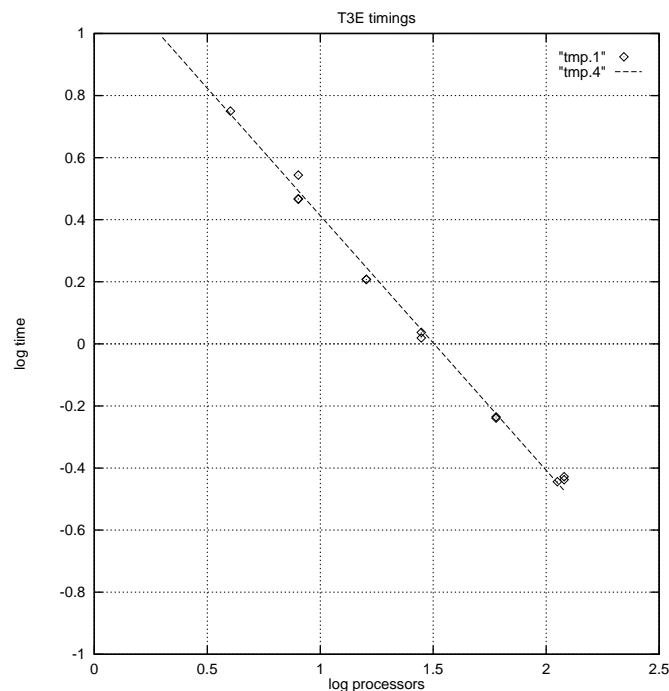
⇒ domain decomposition, guard cells, message passing:



⇒ extra nodes for: ionosphere(1), I/O(1), restart file manager(1), and for things to come

Computer issues (continued)

- ⇒ runs on IBM/SP2, CRAY/T3E, workstation (Beowulf) cluster, ...
- ⇒ language: f77, macro preprocessor, spag, ftnchek.
- ⇒ f90/HPF not mature enough and/or generally available, would require rewriting the code.
- ⇒ using MPI message passing library, either native or MPICH.
- ⇒ excellent scalability:



- ⇒ computing chore: ~ 2000 Flop/gridpoint/timestep.
- ⇒ current machines: ~ 100 MFlop/s.
- ⇒ realtime: 60 nodes, 10^6 cells.
- ⇒ output: several GB per run.

Things to do, given unlimited time and resources

- Adding more physics: inner magnetosphere, ring current

⇒ bounce averaged drift equations:

$$\begin{aligned} \frac{d\lambda_k}{dt} &= \left(\frac{\partial}{\partial t} + \mathbf{v}_k \cdot \nabla \right) \lambda_k = && 0 \\ \frac{d\eta_k}{dt} &= \left(\frac{\partial}{\partial t} + \mathbf{v}_k \cdot \nabla \right) \eta_k = && 0 \\ \mathbf{v}_k &= B^{-2} q_k^{-1} (q_k \mathbf{E} \times \mathbf{B} + \lambda_k \mathbf{B} \times \nabla V^{-2/3}) \\ \lambda_k &= && W_k V^{2/3} \\ \eta_k &= && n_k V \\ V &= && \int ds / B \end{aligned}$$

[Harel et al., 1981; Wolf et al., 1983; 1991; 1993]

⇒ magnetic field: dipole,

⇒ plasma represented by macroparticles of constant λ_k and η_k

⇒ 32 log spaced energy levels, 0.1 to 300 keV

⇒ currently one species: protons

⇒ plasma loss due to pitch angle scattering: 10% of strong pitch angle scattering limit for protons

⇒ plasma loss due to charge exchange with exospheric hydrogen: [Smith and Bewtra, 1978; Anderson et al., 1987]

Things to do (continued)

- Inner magnetosphere (continued)

⇒ plasma loss due to Coulomb drag with plasmaspheric electrons: [*Fok et al., 1991*]

⇒ 10° by $0.1 R_E$ grid in the magnetic equator, $1.2 \leq L \leq 7$

⇒ 0.1 to 0.5 million macroparticles per species, 1 processor

⇒ long timesteps (≈ 1 minute)

Things to do (continued)

- Coupling with thermosphere - ionosphere circulation models (CTIM, TIECGM,

⇒ need: ionospheric parameters (j_{\parallel} , precipitation)

⇒ provide: better ionospheric conductances, potential (neutral wind coupling, flywheel effect), ionospheric outflow.

- Resolution, resolution, resolution

⇒ basic scaling law: $T \sim N^4 = h^{-4}$, but computer power grows exponentially with time:

